Demonstration Of Phase Contrast In Scanning Transmission X-ray Microscopy: Comparison Of Images Obtained At NSLS X1-A With Numerical Simulations

François Polack[1], Denis Joyeux[2], Michael Feser[3], Daniel Phalippou[2], Mary Carlucci-Dayton[3], Konstantyn Kaznacheyev[3], and Chris Jacobsen[3]

[1] *LURE, bât. 209 D , Centre Universitaire Paris XI, BP 34, F-91898 ORSAY Cedex - FRANCE*
[2] *Laboratoire Charles Fabry, Institut d'Optique - BP 147 - 91403 Orsay, FRANCE*
[3] *Physics Department, State University of New York at Stony Brook, Stony Brook, NY , USA*

Abstract. Unlike transmission X-ray microscopy, scanning transmission X-ray microscopy (STXM), till now, does not allow phase contrast. Several method have been suggested but no proof of practical feasibility has been yet given. Here we analyze the methods based on the detection of the small beam deflection induced by the object phase gradient, by a segmented detector. It is shown that structuring the zone plate illumination potentially improves the detection. A diffractive beam profiler has been constructed to condition the beam of the NSLS X1A STXM. Recent images are shown, which, compared to numerical simulations, indicate the presence of phase contrast

INTRODUCTION

Compared to transmission X-ray microscopy (TXM), scanning transmission microscopy (STXM) has till now the obvious disadvantage that it does not allow phase contrast. Phase contrast has however been successfully applied to TXM, and the published images clearly reveal the potential advantages of this type of imaging[1]. Biological materials have usually very similar chemical compositions. Small objects embedded in a closely related matrix may not appear by absorption contrast only, while adding a contrast related to the phase difference may reveal their presence.

Moreover, specimen damage due to the absorbed radiation dose is one of the big issues in X-ray microscopy. The only way to reduce this dose is to base the image formation on a contrast mechanism different from absorption. Phase contrast should allow to increase the energy above the usual soft X-ray range, because absorption decreases more rapidly than phase shift.

For all these reasons any method to extend the phase contrast mode to STXM is worth consideration. In this paper we analyze the principles of phase detection in scanning microscopy, and describe the progress made on an approach based on structured illumination of the pupil and segmented detection in the object far field.

PRINCIPLE OF DIFFERENTIAL PHASE CONTRAST

The detection of the phase shift induced by an object can be done by two main ways, Zernike phase contrast and differential phase contrast (also often called Nomarski phase contrast). In the first case, one detects the phase difference between the object-diffracted and undiffracted light. This is possible with an imaging microscope because in the backfocal plane of the objective, i.e. the Fourier plane, the contributions of different spatial frequencies are separated and can be selectively phase shifted. It cannot of course be applied to a scanning microscope where the signal is detected directly behind the object.

In the second case, local phase gradients are detected through the small phase shift between two close points of the sample. This principle can still be applied to a scanning microscope without an imaging objective, though the implementation has to be rather different from the original Nomarski scheme.

Detection Of Phase Contrast In A Scanning Microscope

In a scanning microscope only a small region of the object is illuminated. If the object has a local phase gradient, it acts as a small prism and the emerging beam is slightly deflected from the position where it stands when no object is present (figure 1.). This deflection can be detected by segmented detector as proposed in references 2 to 4. However, the deflection angle is usually small with respect to the aperture angle that is required to achieve a high resolution. Considering an image, critically sampled with a pixel size roughly equal to the resolution element, the phase gradient required to shift the beam of half its diameter is $\lambda/4$ per pixel. To give an idea of the object modulation, this value corresponds, for a biological object at $\lambda \approx$ 3nm, to a thickness variation around 0.5 µm per pixel. It is therefore reasonable to look for maximum sensitivity to small deflections.

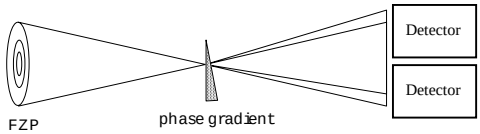

FIGURE 1. Detection of phase gradient in the STXM. The beam may have a particular intensity profile to help the detection of small beam shift by the segmented detector.

Another approach, is to go back the Nomarski scheme and consider two close points of the object. We suppose that we are able to illuminate them with two wavefronts having a constant phase relationship. This statement implies that in the far field, as well upstream as downstream from the focal plane, the complex amplitude inside the pupil aperture, is modulated by a cosine fringe. Now, if we introduce a sample which slightly changes the phase relationship by $\Delta\varphi$, then in the far field the fringe is shifted by a fraction of the period equal to $\Delta\varphi/2\pi$. Small shifts are better detected on the sides of the fringe where the intensity gradient is the larger[5,6]. In référence 6, we previously

suggested to modulate the amplitude incoming on the zone plane by a cosine fringe having a maximum in the center of the zone plate and a period of about 1.6 times the zone plate diameter (period of the intensity pattern, p =0.8 D). The detection is made differentially with two detectors of width p/3, separated by a blind region of same width.

It is obvious that the two point description is a view of the mind and that there is a limited but continuous zone of illumination in the focal plane. If the object phase gradient is uniform in this region, the fringe shift and the pupil shift are the same; if it is locally modulated the pupil and fringe pattern is distorted and becomes the convolution of the pupil illumination by the diffraction pattern of the local modulation. The two detection scheme actually differ by the way the useful signal is distributed in the pupil plane as shown in the next paragraph.

First Order Signal Analysis

We consider here that by use of a convenient beam profiler, the zone plate is illuminated by a definite complex amplitude. We denote $P(\boldsymbol{\theta})$ the complex amplitude distribution in the zone plate pupil plane. The object illumination is the Fourier transform of $P(\boldsymbol{\theta})$ that we denote $\tilde{P}(\mathbf{x})$. We assume that the $P(\boldsymbol{\theta})$ spatial modulation is slow enough that the spot size is not significantly increased with respect to the uniform illumination. We also assume that the object is weakly modulated and this modulation is also slowly varying, so that the object transmittance can be developed to the first order in the illuminated region as

$$T(\mathbf{x}) = 1 - O(\mathbf{x}_0 + \mathbf{x}) = 1 - O(\mathbf{x}_0) + \mathbf{x} \cdot \nabla O(\mathbf{x}_0) + 2^{nd}\, order \qquad 1$$

where $\mathbf{x}$ is the space variable in the zone plate focal plane, $O(\mathbf{x})$ is the object modulation in amplitude, $O(\mathbf{x}) << 1$, and $\mathbf{x}_0$ is the point of the object which is located at the center of the X-ray spot during the considered step of the scanning process.

Just behind the object, the complex amplitude is the product $\tilde{P}(\mathbf{x})T(\mathbf{x})$, and we obtain the amplitude $D(\boldsymbol{\theta})$ in the detector plane by a Fourier transform with respect to the variable $\mathbf{x}$ **:**

$$D(\theta) = TF\left\{\tilde{P}(\mathbf{x})\left[1 - O(\mathbf{x}_0)\right] - \tilde{P}(\mathbf{x})\,\mathbf{x} \cdot \nabla O(\mathbf{x}_0)\right\} \qquad 2$$

Which, using the properties of derivation of the Fourier transform can be rewritten as:

$$D(\theta) = P(\theta)\left[1 - O(\mathbf{x}_0)\right] - \frac{\lambda}{2i\pi} \nabla P(\theta) \cdot \nabla O(\mathbf{x}_0) \qquad 3$$

Finally the intensity is obtained by squaring the amplitude and, with a weak object, we can neglect second order terms in $O(\mathbf{x}_0)$ and $\nabla O(\mathbf{x}_0)$, and get :

$$\left|\mathrm{D}(\theta)\right|^2 = \left|\mathrm{P}(\theta)\right|^2 \left\{1 - 2\,\mathrm{Re}\left[\mathrm{O}(\mathbf{x}_0)\right]\right\} - \frac{\lambda}{\pi}\,\mathrm{Im}\left[\mathrm{P}^*(\theta)\,\nabla\mathrm{P}(\theta)\cdot\nabla\mathrm{O}(\mathbf{x}_0)\right] + 2^{nd}\ order \quad 4$$

In order to better distinguish the behavior of the real and imaginary parts of the object modulation, we let appear the amplitude and phase of the pupil function and their gradients with :

$$\mathrm{P}(\theta) = \left|\mathrm{P}(\theta)\right| e^{i\phi(\theta)}; \qquad \nabla\mathrm{P}(\theta) = \nabla\left|\mathrm{P}(\theta)\right| e^{i\phi(\theta)} + i\,\mathrm{P}(\theta)\nabla\phi(\theta) \quad 5$$

Hence :

$$\left|\mathrm{D}(\theta)\right|^2 = \left|\mathrm{P}(\theta)\right|^2 \left\{1 - 2\,\mathrm{Re}\left[\mathrm{O}(\mathbf{x}_0)\right] - \frac{\lambda}{\pi}\,\mathrm{Re}\left[\nabla\mathrm{O}(\mathbf{x}_0)\right]\cdot\nabla\phi(\theta)\right\} - \frac{\lambda}{2\pi}\,\nabla\left|\mathrm{P}(\theta)\right|^2\cdot\mathrm{Im}\left[\nabla\mathrm{O}(\mathbf{x}_0)\right] \quad 6$$

Thus, the signal received in the detection plane has three components. The first one is proportional to the local intensity transmission factor of the object and the pupil intensity, it could be called the normal signal. The second signal is proportional to the real part of the object gradient, the pupil phase gradient and the pupil intensity. This signal appears for instance when the zone plate is out of focus or if individual zones are not perfectly registered. The third signal is the phase signal we are looking for; it is proportional to the object phase gradient and the gradient of the pupil intensity.

Optimum Detection Scheme

The signal distribution is quite different in the two detection schemes we have considered. In the first case, the pupil is uniform and the phase signal is only located on the pupil edge. Zone plates are usually not as perfect on the outside as in the center, because placement errors are more likely to happen at high frequency. These phase gradients may bring in some parasitic amplitude signal.

On the contrary if the pupil intensity is modulated by a sine fringe with a maximum symmetrically centered with a maximum on the zone plate axis, the intensity gradient is more evenly distributed. The signal can be integrated on a larger area, therefore a larger fraction of the energy contributes to the signal. The regions of maximum signal are also located in the mid-frequency range of the zone plate where the pattern is expected to be more accurate. The functions $\left|\mathrm{P}(\theta)\right|^2$ and $\nabla\left|\mathrm{P}(\theta)\right|^2$ which modulate the local contribution of the intensity and phase signals are respectively even and odd. Two identical detectors are symmetrically disposed in the detection plane and therefore the intensity signal is obtained as the sum of the detector signals and the phase signal as their difference.

The geometry of the detection can be optimized to get the maximum phase signal. When the circular shapes of the zone plate and of its central obstruction are taken into

account, one obtains the parameters we have already given. These parameters however are not critical.

BEAM PROFILING TECHNIQUES

Young's fringes

In a STXM, the zone plate is illuminated by a coherent wavefront. It is thus possible to produce the desired sine fringe by the diffraction from a pair of slits, inserted at some distance upstream the zone plate. This set up was used for the first experiments we did on the X1A microscope at NSLS. In order to obtain the proper fringe period, the two slits were set at 570 mm from the zone plate. The slit width were 18 µm and they were separated by a 18 µm wide opaque region. Though it was possible to see the fringe shift with this set-up, it was not stable enough to get differential images. The X1A STXM is supported by an air suspended table, but due to the distance it was not possible to attach the slits to the same table. With the set up parameters a relative displacement of 1 µm between the slit and the zone plate produces a spurious signal equivalent to a phase shift of $\lambda/40$.

Diffractive Beam Profiler

For the most recent experiments, a new beam profiler has been constructed. It is based on the variation of the 0^{th} order efficiency of a binary grating, versus the groove duty cycle. When the phase shift due to the groove depth is π, this efficiency is related to the duty cycle, c (defined as the groove width to period ratio) by :

$$E_0 = \frac{1-2c}{2\pi}, \quad c \in [0,1] \qquad 7$$

The wanted continuous and signed amplitude modulation, can be obtained by modulating the line width (LW) of a high carrier frequency binary grating. The construction parameters are the following: Carrier period 46 µm, period of LW modulation 7.4 mm, ruled length 24 mm. The grating is used in grazing reflection at 1 deg, in the 2 to 4.5 nm wavelength range. The minimum distance at which the orders are separated is 100 mm; it is actually set at 400 mm from the zone plate, but is rigidly linked to the microscope table. The grating was designed in order that under parallel illumination the period of projected modulation is 66 µm, adapted to a 80 µm diameter ZP. Unfortunately the beam from the monochromator is diverging, so that the projected period is actually 100 µm.

The grating beam-profiler is incorporated in an assembly of four reflectors (figure 2). The grating is RIE etched in a layer of amorphous silicon. It does not occupy the whole

width of the blank, but leaves a 5 mm reflecting track which can be used to reject the higher harmonics from the monochromator. The thickness of the Si layer varies from 28 nm on one side of the grating to 74 nm on the other. For each wavelength, the best modulation (π phase shift) is achieved by the translation of the whole device. The 15 mm tracks of the grating and mirrors which are used with the beam profiler are nickel coated. On the harmonic rejection path, the external. mirrors (1deg grazing) are chromium coated, the internal ones (3deg grazing) are bare silica.

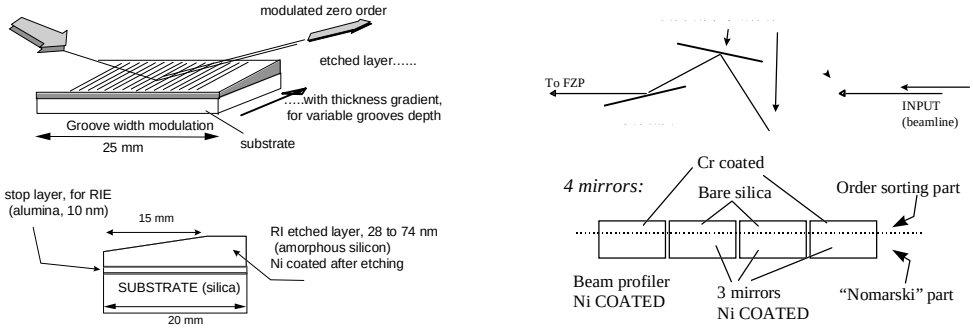

FIGURE 2. Principle of the beam profiler and schematics of the harmonics rejection device

EXPERIMENTS

Demonstrating a phase contrast in soft X-ray is not an easy task because materials are both absorber and phase shifter. The influence of parasitic amplitude signal can be reduced if the sample is immersed in a medium of comparable absorption coefficient but different refractive index. Such a close match occurs for instance with silica and toluene in the 2.5 to 2.6 nm wavelength range.

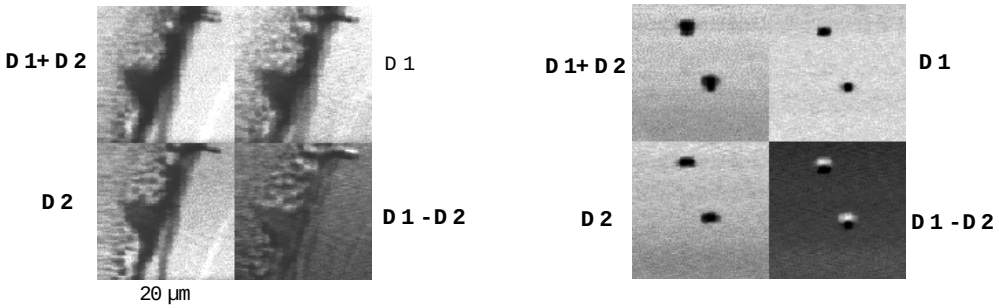

FIGURE 3. STXM images of 2µm diameter silica spheres in toluene. Left group: cluster of several spheres; right group: two isolated spheres. Individual images show the D1 and D2 detector signals and their combinations, D1+D2 is the amplitude signal, D1-D2 is the phase signal.

We used silica beads (1- 2 µm diameter), and maintained them in toluene between two sealed Si_3N_4 membranes. 2µm thick silica alone has a transmission factor of ~ 10% and a 1.1 λ optical thickness. In toluene the transmission difference is only a few percent, but the difference in optical thickness is still 0.5 λ. The sample however is

difficult to manipulate. Capillary forces tends to exclude toluene from the center of the window. It is useful to reduce the thickness of the liquid layer, but the nitride membranes cannot withstand the stress for a long time. We have been able to make only a few images. The resolution is low because we were the first user of the new STXM and the piezo scanning stage was not yet available. Two regions of the sample are shown on figure 4., one with a cluster of silica spheres, the other with two isolated ones. Both images are 100 x 100 points with .2 µm pixels. Four views of each region are shown corresponding to the signal of each detector, their sum and their difference. On the difference one can see the contrast reversal which is characteristic of differential phase contrast.

COMPARISON WITH NUMERICAL SIMULATIONS

To convince ourselves that the contrast we see is actually due to phase shifts, we made computer simulation of the image which are expected from these simple objects in various situations. The computation procedure is rather straightforward.

1) The pupil illumination defined by the zone plate geometry and the fringe period is sampled on a 128 x128 complex array, and Fourier transformed to obtain the sample illumination

2) For one particular position of the object with respect to the probe, the sample illumination is multiplied by the complex transmission factor of the object, and the result is Fourier transformed to obtain the complex amplitude in the detection plane.

3) The intensity is computed and integrated on each detector window.

The sample is then moved to the next pixel and step 2 and 3 are repeated until the whole image is computed.

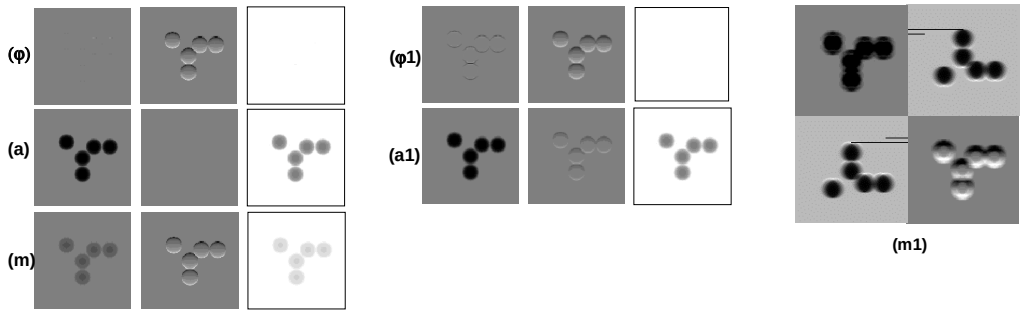

FIGURE 4. Simulated images of a pattern of 5 spheres of 2µm diameter in a 12 µm field. In the two left groups (φ to a1) the 1st column is the detector sum D1+D2 (amplitude), the 2nd column is the difference D1-D2 (phase), and the 3rd column is the image in normal transmission mode: **φ)** pure phase object, λ/2 maximum phase shift; **a)** pure amplitude, object minimum transmission 50%; **m)** mixed contrast as silica spheres in toluene, max. phase shift λ/2, minimum transmission 85%; **φ1)** and **a1)** same as φ) and a), but the probe is out of focus by 3µm; **m1)** shows the simulated 4 signals from silica spheres not immersed in toluene, out of focus by 6 µm; same image arrangement as in figure 3.

Figure 4 shows the results in some particular conditions. First we look at pure phase and amplitude objects with a probe in perfect focus, phase and amplitude images are

perfectly discriminated as well with pure phase or amplitude objects (φ/ and a/ images) as with a sample presenting a mixed contrast like silica spheres in toluene (m). The contrast reversed features which appears in the phase images have a higher resolution in the simulation than on the STXM image. This is an indication the STXM was out of focus.
The second, set of images simulates what happen when the probe is defocused by 3µm. While the 1st order analysis says the signal remains perfectly discriminated, the simulations show a weak cross-talk signal. This signal, however, cannot explain by itself the observed contrast in the phase image even for a larger defocusing.
The last image simulate the case of a dried-up sample of silica spheres without toluene and a strong 6 µm defocusing. The phase image looks quite similar to the STXM image but the contrast of the amplitude image is stronger on the simulation. We therefore conclude that our images are actual phase images, taken with a rather out of focus probe and that our sample suffered from some loss of toluene.

CONCLUSION

It has been shown that in the first order approximation, three object related terms are present in the detection plane of a STXM, the intensity transmission factor, and the real and imaginary part of the gradient of the complex transmission. According to the illumination of the zone plate, these terms have different symmetry of distribution and can be separately recorded by segmented detectors. An optimized detection scheme was described which includes, for stability, a 0th order diffractive beam profiler to modulate the zone plate illumination. Preliminary images have been compared to computer simulations. The contrast observed can only be explained by the presence of a phase contribution.

REFERENCES

1. Schmahl, G., Guttmann, P., Schneider, G., Thieme, J., Niemann, B., and Wilhein, T., *Synchrotron radiation News*, **7**, 19-22,. (1994)

2. Morrison, G. R., « Phase Contrast and Darkfiel Imaging in X-ray Microscopy »,in *Soft X-ray Microscopy*, edited by C. J. Jacobsen and J. E. Trebes, Proc.SPIE 1741, 1992, pp. 186-193

3. Morrison, G. R. and Niemann, B., « Differential Phase Contrast X-Ray Microscopy», in: *X-ray Microscopy and Spectromicroscopy*, edited by J. Thieme et al., Springer Verlag, 1998, pp. I-855 - I-94

4. Kirz, J., Jacobsen, C., and Howells, M., *Quarterly Reviews of Biophysics* **28**, 33-130 (1995)

5. Polack, F., and Joyeux, D., « Soft X-ray interferential microscopy: a feasibilityassessment » in: *X-ray Microscopy IV*, edited by A. I. Erko and V. V. Aristov, Bogorodski Pechatnik, Chernogolovka, 1994

6. Polack, F., Joyeux D., and Phalippou,D.,« Phase Contrast Experiments on the NSLS-X1A Scanning Microscope », in: *X-ray Microscopy and Spectromicroscopy*, edited by J. Thieme et al., Springer Verlag, 1998, pp. I-105 - I-110

7 Joyeux, D., and Polack, F., « A Wavefront Profiler as an Insertion Device for Scanning Phase Contrast Microscopy », in: *X-ray Microscopy and Spectromicroscopy*, edited by J. Thieme et al., Springer Verlag, 1998, pp. II-201 - II-206